Journal of Engineering Mathematics **49:** 99–112, 2004.

A linear differential equation with a time-periodic damping coefficient: stability diagram and an application

HARTONO* and A.H.P. VAN DER BURGH
Department of Applied Mathematical Analysis, Faculty of Information Technology and Systems, Delft University of Technology, Mekelweg 4, 2628 CD Delft, The Netherlands

Received 8 April 2002; accepted in revised form 27 September 2003

Abstract. In this paper the second-order differential equation with time-dependent damping coefficient

$$\ddot{x} + \epsilon \cos(2t)\dot{x} + \lambda x = 0, \tag{0.1}$$

will be studied. In particular the coexistence of periodic solutions corresponding with the vanishing of domains of instability is investigated. The coexistence of π-periodic solutions occurs for $\lambda \approx 4n^2$ where n is integer. This implies that the instability area which is emanating from $\lambda = 4n^2$ in the $\lambda - \epsilon$ stability diagram disappears. In applications, this equation can be considered as a model equation for the study of rain-wind-induced vibrations of a special oscillator.

Key words: coexistence, rain-wind-induced vibrations, stability diagram, time-periodic damping coefficient

1. Introduction

In this paper we consider an inhomogeneous second-order differential equation with time-dependent damping coefficient, *i.e.*,

$$\ddot{x} + (c + \epsilon \cos(2t))\dot{x} + (m^2 + \alpha)x + A \cos \omega t = 0, \tag{1.1}$$

where c, α, ϵ, A are small parameters and m, ω positive integers. A rather special property of Equation (1.1) is that the coefficient of $\dot{x}$ is time-dependent. For $m = 1$ and $A = 0$ some results especially related to the stability of the trivial solution can be found in [1]. The result of the stability diagram of periodic solution of Equation (1.1) for $m = 3$ are presented in [2]. Further for the case $c = 0$ and $A = 0$ the Equation (1.1) is a special case of Ince's equation (see [3, page 92], *i.e.*, $a = 0$, $d = 0$ and $t \to t + \pi/4$). It is known that Ince's equation displays the phenomenon of coexistence of periodic solutions when m is an even integer. Coexistence implies that domains of instability disappear or, in other words, that an instability gap closes. The coexistence of periodic solutions of this equation will be studied in this paper. A new stability diagram is presented and a strained parameter is used to obtain approximations for the transition and the coexistence curves for small value of ϵ. Finally it is shown that (1.1) can be used as a model equation for the study of rain-wind-induced vibrations of a special oscillator.

*Lecturer in Jurusan Matematika Universitas Negeri Yogyakarta, Indonesia, on leave as a PhD reseacher at Delft University of Technology, The Netherlands.

2. Coexistence of time-periodic solutions and the stability diagram

For the case $c = A = 0$ and replacing $m^2 + \alpha$ by λ, Equation (1.1) can be written as

$$\ddot{x} + (\epsilon \cos(2t))\dot{x} + \lambda x = 0. \tag{2.1}$$

Transform x to the new variable y by

$$x = y \cdot \mathrm{e}^{-\frac{1}{2}\int_0^t \epsilon \cos(2s)\mathrm{d}s} \tag{2.2}$$

to obtain a new equation of Hill's type:

$$\ddot{y} + (\lambda - \frac{1}{8}\epsilon^2 + \epsilon \sin(2t) - \frac{1}{8}\epsilon^2 \cos(4t))y = 0. \tag{2.3}$$

The standard form of Hill's equation (in [6]) is

$$\ddot{y} + [\lambda + Q(t)]y = 0, \tag{2.4}$$

where λ is a parameter and Q is a real π-periodic function in t. Apparently (2.3) is of type (2.4) where $Q(t)$ depends additionally on a parameter ϵ. The determination of the value of λ for which Equation (2.4) has a π or 2π periodic solution can be related to the following theorem:

Theorem [3, p. 11]

To every differential Equation (2.4), there belong two monotonically increasing infinite sequences of real numbers $\lambda_o, \lambda_1, \lambda_2, \cdots$ and $\lambda_1', \lambda_2', \lambda_3', \cdots$ such that (2.4) has a solution of period π if and only if $\lambda = \lambda_n, n = 0, 1, 2, \cdots$ and a solution of period 2π if and only if $\lambda = \lambda_n', n = 1, 2, 3, \cdots$. λ_n and λ_n' satisfy the inequalities

$$\lambda_o < \lambda_1' \leq \lambda_2' < \lambda_1 \leq \lambda_2 < \lambda_3' \leq \lambda_4' < \lambda_3 \leq \lambda_4 < \cdots$$

and the relations

$$\lim_{n\to\infty} \lambda_n^{-1} = 0, \qquad \lim_{n\to\infty} (\lambda_n')^{-1} = 0.$$

The solutions of (2.4) are stable[1] in the intervals

$$(\lambda_o, \lambda_1'), (\lambda_2', \lambda_1), (\lambda_2, \lambda_3'), (\lambda_4', \lambda_3), \cdots.$$

At the endpoints of these intervals the solutions of (2.4) are, in general, unstable. The solutions of (2.4) are stable for $\lambda = \lambda_{2n+1}$ or $\lambda = \lambda_{2n+2}$ if and only if $\lambda_{2n+1} = \lambda_{2n+2}$, and they are stable for $\lambda = \lambda_{2n+1}'$ or $\lambda = \lambda_{2n+2}'$ if and only if $\lambda_{2n+1}' = \lambda_{2n+2}'$.

As described in [3, p. 90], Hill's equation in general has only one periodic solution of period π or 2π. If the equation has two linearly independent solutions of period π or 2π, we say that two such solutions *coexist*. Every solution of this equation can then be expressed in a linear combination of two periodic solutions, in other words, all solutions are bounded or they are stable. Thus the occurrence of coexisting periodic solutions is equivalent with the disappearance of intervals of instability. If, for instance, two linearly independent solutions of period π exist, then the interval of instability $(\lambda_{2n+1}, \lambda_{2n+2})$ disappears, because $\lambda_{2n+1} = \lambda_{2n+2}$.

[1] All solutions of (2.4) are bounded

Further in [4] a special case of $Q(t)$ was studied, that is, if $Q(t)$ in Equation (2.4) has the form

$$Q(t) = \lambda_o + \dot{P}(t) + P^2(t), \tag{2.5}$$

where $P(t)$ is $\pi/2$-anti-periodic i.e. $P(t + \pi/2) = -P(t)$, then $\lambda_{2n+1} = \lambda_{2n+2}$ for all n.

Clearly Equation (2.3) is of the form (2.5) with $P(t) = -\frac{1}{2}\epsilon \cos 2t$ and $\lambda_o = 0$, and $\cos 2t$ is $\pi/2$ anti-periodic. Thus coexistence in Equation (2.3) exists for $\lambda = \lambda_{2n+1} = \lambda_{2n+2}$. Unfortunately it is not known how to calculate exactly the value of λ for which Equation (2.3) has a periodic solution. However, one can approximate the value of λ by the following method [5].

We consider a Fourier-series representation of the periodic solution:

$$y = \frac{a_o}{2} + \sum_{n=1}^{\infty}(a_n \cos nt + b_n \sin nt). \tag{2.6}$$

Substituting (2.6) in (2.3) yields

$$\begin{aligned}
&(\lambda - \tfrac{1}{8}\epsilon^2)\tfrac{a_o}{2} + \epsilon\tfrac{a_o}{2}\sin 2t - \tfrac{1}{16}\epsilon^2 a_o \cos 4t + \\
&\textstyle\sum_{n=1}^{\infty}[(\lambda - \frac{1}{8}\epsilon^2 - n^2)a_n \cos nt + (\lambda - \frac{1}{8}\epsilon^2 - n^2)b_n \sin nt] + \\
&\tfrac{1}{2}\epsilon \textstyle\sum_{n=1}^{\infty}[a_n \sin(n+2)t - a_n \sin(n-2)t - b_n \cos(n+2)t + b_n \cos(n-2)t] \\
&-\tfrac{1}{16}\epsilon^2 \textstyle\sum_{n=1}^{\infty}[a_n \cos(n+4)t + a_n \cos(n-4)t + b_n \sin(n+4)t + b_n \sin(n-4)t] = 0.
\end{aligned} \tag{2.7}$$

Equating the coefficients of sine and cosine functions to zero, we have a system of infinitely many equations for a_n and b_n. In this way we obtain a system that can be split into two systems *i.e.*,

$$\mathbf{A}(\lambda, \epsilon)\mathbf{v} = \mathbf{0} \qquad \text{and} \qquad \mathbf{B}(\lambda, \epsilon)\mathbf{w} = \mathbf{0},$$

where $\mathbf{A}(\lambda, \epsilon)$, $\mathbf{B}(\lambda, \epsilon)$ are square matrices of infinite dimension and $\mathbf{v}$ is an infinite column vector where the elements are coefficients of (2.6) with odd indices and $\mathbf{w}$ is an infinite column vector where the elements are coefficients of (2.6) with even indices. The odd indices correspond to 2π-periodic solutions and the even indices correspond to π-periodic solutions of Equation (2.3). To have a non-trivial solution, the determinants of $\mathbf{A}$ and $\mathbf{B}$ must be equal zero. These determinants define the curves in the $\epsilon - \lambda$ plane on which periodic solutions exist. However, it is not possible to compute these curves from the determinants, as they are of infinite dimension. Hence we consider (2.6) and truncate the series up to 16 modes from which determinants of finite dimension follow. From a technical point of view, it follows that, if more modes are added the result will be more accurate. It will be seen later that this result for small values of ϵ and that obtained by using the strained-parameter method up to order ϵ^8 coincide. For example, the case $\epsilon = 1$ is presented in Table 1. In the determinants we choose ϵ from the interval $(0, 24)$ arbitrary but fixed. Subsequently the determinants are evaluated yielding an algebraic equation for λ that can be solved numerically. In this way a new stability diagram as depicted in Figure 1b is obtained. In a similar way the famous stability diagram of the Mathieu equation:

$$\ddot{y} + (\lambda + \epsilon \cos(2t))y = 0 \tag{2.8}$$

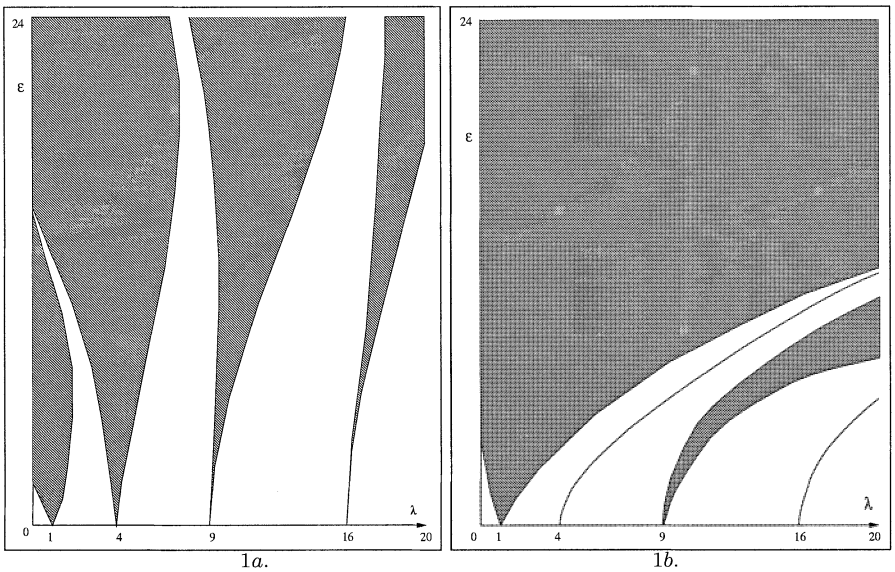

1*a*. 1*b*.

Figure 1. In the shaded regions the trivial solution is unstable. On the curves separating the white and shaded regions periodic solution exist. Figure 1a the Mathieu stability diagram. Figure 1b the new stability diagram.

is obtained and presented in Figure 1a. One can observe remarkable differences between the two diagrams. Especially the curves starting in $\lambda = 4n^2$, $n = 1, 2, 3, \cdots$ on which two periodic solutions coexists are of interest.

When ϵ is small, we can use the strained parameter method, as described in [6], to approximate the value of λ for which Equation (2.3) has periodic solutions. In this method we assume that λ can be expanded as

$$m^2 + \epsilon\alpha_1 + \epsilon^2\alpha_2 + \epsilon^3\alpha_3 + \cdots, \tag{2.9}$$

where m is an integer number and the solution of (2.3) is expanded as

$$a_o \cos mt + b_o \sin mt + \epsilon y_1(t) + \epsilon^2 y_2(t) + \epsilon^3 y_3(t) + \cdots. \tag{2.10}$$

Substituting (2.10) in (2.3) and eliminating the secular terms we obtain the values of α_i, $i = 1, 2, 3, \cdots$. For instance, for $m = 1$ we obtain $a_o = -b_o$ and $\lambda = \lambda_1'$ where

$$\begin{aligned} \lambda_1' &= 1 - \tfrac{1}{2}\epsilon + \tfrac{3}{32}\epsilon^2 - \tfrac{3}{512}\epsilon^3 - \tfrac{3}{8192}\epsilon^4 + \tfrac{5}{141072}\epsilon^5 \\ &\quad - \tfrac{17}{4194304}\epsilon^6 - \tfrac{7}{134217728}\epsilon^7 - \tfrac{1}{16777216}\epsilon^8 + O(\epsilon^9) \end{aligned} \tag{2.11}$$

or $a_o = b_o$ and $\lambda = \lambda_2'$ where

$$\begin{aligned} \lambda_2' &= 1 + \tfrac{1}{2}\epsilon + \tfrac{3}{32}\epsilon^2 + \tfrac{3}{512}\epsilon^3 - \tfrac{3}{8192}\epsilon^4 - \tfrac{5}{141072}\epsilon^5 + \\ &\quad \tfrac{17}{4194304}\epsilon^6 + \tfrac{7}{134217728}\epsilon^7 - \tfrac{1}{16777216}\epsilon^8 + O(\epsilon^9). \end{aligned} \tag{2.12}$$

But for $m = 2$, we obtain $b_o = 0$ and $\lambda = \lambda_1$ or $a_o = 0$ and $\lambda = \lambda_2$ where $\lambda_1 = \lambda_2$, *i.e.*,

$$\lambda_1 = 4 + \tfrac{1}{6}\epsilon^2 - \tfrac{1}{3456}\epsilon^4 - \tfrac{1}{1244160}\epsilon^6 + \tfrac{11}{5733089280}\epsilon^8 + O(\epsilon^9). \tag{2.13}$$

Table 1. Comparison of the values of λ obtained with the numerical and the perturbation method for $\epsilon = 1$.

Numerical	Analytical
$\lambda_1' = 0{\cdot}5875\mathbf{66498}$	$0{\cdot}5875\mathbf{55692}$
$\lambda_2' = 1{\cdot}5992\mathbf{09067}$	$1{\cdot}5992\mathbf{11767}$
$\lambda_1 = 4{\cdot}166376513$	$4{\cdot}166376513$
$\lambda_3' = 9{\cdot}134927\mathbf{378}$	$9{\cdot}134927\mathbf{383}$
$\lambda_4' = 9{\cdot}146588\mathbf{994}$	$9{\cdot}146588\mathbf{991}$
$\lambda_3 = 16{\cdot}13343594$	$16{\cdot}13343594$

For $m = 3$ we proceed similarly as for $m = 1$, that is, we obtain $a_o = b_o$ and $\lambda = \lambda_3'$ where

$$\begin{aligned}\lambda_3' \;=\; & 9 + \tfrac{9}{64}\epsilon^2 - \tfrac{3}{512}\epsilon^3 + \tfrac{9}{65536}\epsilon^4 + \tfrac{15}{524288}\epsilon^5 \\ & - \tfrac{141}{33554432}\epsilon^6 - \tfrac{21}{536870912}\epsilon^7 + \tfrac{4101}{68719476736}\epsilon^8 + O(\epsilon^9),\end{aligned} \tag{2.14}$$

or $a_o = -b_o$ and $\lambda = \lambda_4'$ where

$$\begin{aligned}\lambda_4' \;=\; & 9 + \tfrac{9}{64}\epsilon^2 + \tfrac{3}{512}\epsilon^3 + \tfrac{9}{65536}\epsilon^4 - \tfrac{15}{524288}\epsilon^5 \\ & - \tfrac{141}{33554432}\epsilon^6 + \tfrac{21}{536870912}\epsilon^7 + \tfrac{4101}{68719476736}\epsilon^8 + O(\epsilon^9).\end{aligned} \tag{2.15}$$

The case $m = 4$ is similar to that for with $m = 2$. We obtain $b_o = 0$ and $\lambda = \lambda_3$ or $a_o = 0$ and $\lambda = \lambda_4$ with $\lambda_3 = \lambda_4$ i. e.

$$\lambda_3 = 16 + \tfrac{2}{15}\epsilon^2 + \tfrac{11}{108000}\epsilon^4 + \tfrac{1033}{1360800000}\epsilon^6 - \tfrac{60703}{31352832000000}\epsilon^8 + O(\epsilon^9). \tag{2.16}$$

The approximations of λ_1' and λ_2' are given by (2.11) and (2.12), respectively. The approximations of λ_1 and λ_2 are the same and are given by (2.13). The expansions of λ_3' and λ_4' are given by (2.14) and (2.15), respectively, and finally the approximations of λ_3 and λ_4 are given by (2.16).

The analytical results as obtained above are compared with the numerical results as presented in Figure 1b, for $\epsilon = 1$ in Table 1. One can observe a striking resemblance. The occurrence of the coexistence of periodic solutions in Equation (2.3) depends on the periodicity of the coefficient of the damping term. It is known that coexistence occurs when the coefficient of the damping term is $\pi/2$-anti periodic. So, if one perturbs the period, then coexistence does not occur any longer, as is shown by the following example:

Consider the equation

$$\ddot{x} + (\epsilon\cos(2t) + \epsilon b\cos t)\dot{x} + \lambda x = 0. \tag{2.17}$$

The period of the coefficient of the damping term is 2π if b is not equal zero; thus, if one transforms Equation (2.17) into one of Hill's type, then this equation does not satisfy (2.5), *i.e.*, $P(t + \pi/2) \neq -P(t)$, where $P(t) = -\frac{1}{2}(\epsilon\cos(2t) + \epsilon b\cos t)$. So coexistence does no

longer occur and the approximations of λ_1', λ_2', λ_1, λ_2, λ_3', λ_4', λ_3 and λ_4 (up to order $O(\epsilon^9)$) are given by

$$\begin{aligned}
\lambda_1' \;=\; & 1 - \tfrac{1}{2}\epsilon + (\tfrac{3}{32} + \tfrac{1}{6}b^2)\epsilon^2 - (\tfrac{3}{512} + \tfrac{1}{36}b^2)\epsilon^3 - (\tfrac{3}{8192} + \tfrac{7}{576}\,b^2 + \tfrac{1}{864}\,b^4)\epsilon^4 \\
& + (\tfrac{5}{131072} + \tfrac{11}{3072}\,b^2 + \tfrac{47}{13824}\,b^4)\epsilon^5 \\
& + (\tfrac{17}{4194304} - \tfrac{39}{573440}\,b^2 - \tfrac{653}{4976640}\,b^4 - \tfrac{1}{77760}\,b^6)\epsilon^6 \\
& - (\tfrac{7}{134217728} + \tfrac{187403}{2890137600}\,b^2 + \tfrac{430961}{1194393600}\,b^4 + \tfrac{3877}{18662400}\,b^6)\epsilon^7 \\
& + (-\tfrac{1}{16777216} + \tfrac{6431}{2055208960}\,b^2 + \tfrac{1259837}{17836277760}\,b^4 \\
& + \tfrac{10421}{627056640}\,b^6 + \tfrac{11}{89579520}\,b^8)\epsilon^8 + O(\epsilon^9),
\end{aligned} \tag{2.18}$$

$$\begin{aligned}
\lambda_2' \;=\; & 1 + \tfrac{1}{2}\epsilon + (\tfrac{3}{32} + \tfrac{1}{6}b^2)\epsilon^2 + (\tfrac{3}{512} + \tfrac{1}{36}b^2)\epsilon^3 - (\tfrac{3}{8192} + \tfrac{7}{576}\,b^2 + \tfrac{1}{864}\,b^4)\epsilon^4 \\
& + (\tfrac{5}{131072} + \tfrac{11}{3072}\,b^2 + \tfrac{47}{13824}\,b^4)\epsilon^5 \\
& + (\tfrac{17}{4194304} - \tfrac{39}{573440}\,b^2 - \tfrac{653}{4976640}\,b^4 - \tfrac{1}{77760}\,b^6)\epsilon^6 \\
& - (\tfrac{7}{134217728} + \tfrac{187403}{2890137600}\,b^2 + \tfrac{430961}{1194393600}\,b^4 + \tfrac{3877}{18662400}\,b^6)\epsilon^7 \\
& + (-\tfrac{1}{16777216} + \tfrac{6431}{2055208960}\,b^2 + \tfrac{1259837}{17836277760}\,b^4 + \tfrac{10421}{627056640}\,b^6 \\
& + \tfrac{11}{89579520}\,b^8)\epsilon^8 + O(\epsilon^9),
\end{aligned} \tag{2.19}$$

$$\begin{aligned}
\lambda_1 \;=\; & 4 + (\tfrac{1}{6} + \tfrac{2}{15}\,b^2)\epsilon^2 - \tfrac{1}{36}b^2\epsilon^3 + (-\tfrac{1}{3456} + \tfrac{1}{180}\,b^2 + \tfrac{11}{27000}\,b^4)\epsilon^4 \\
& + (-\tfrac{37}{64800}\,b^2 - \tfrac{1}{1350}\,b^4)\epsilon^5 \\
& - (\tfrac{1}{1244160} + \tfrac{79}{6531840}\,b^2 + \tfrac{6397}{108864000}\,b^4 + \tfrac{1033}{85050000}\,b^6)\epsilon^6 \\
& + (\tfrac{1739}{232243200}\,b^2 + \tfrac{7639}{51030000}\,b^4 + \tfrac{409}{58320000}\,b^6)\epsilon^7 \\
& + (\tfrac{11}{5733089280} - \tfrac{67}{470292480}\,b^2 - \tfrac{19979}{261273600}\,b^4 - \tfrac{864931}{48988800000}\,b^6 \\
& - \tfrac{60703}{489888000000}\,b^8)\epsilon^8 + O(\epsilon^9),
\end{aligned} \tag{2.20}$$

$$\begin{aligned}
\lambda_2 \;=\;& 4+(\tfrac{1}{6}+\tfrac{2}{15}\,b^2)\epsilon^2+\tfrac{1}{36}b^2\epsilon^3+(-\tfrac{1}{3456}+\tfrac{1}{180}\,b^2+\tfrac{11}{27000}\,b^4)\epsilon^4\\
&+(-\tfrac{37}{64800}\,b^2-\tfrac{1}{1350}\,b^4)\epsilon^5\\
&-(\tfrac{1}{1244160}+\tfrac{79}{6531840}\,b^2+\tfrac{6397}{108864000}\,b^4-\tfrac{1033}{85050000}\,b^6)\epsilon^6\\
&-(\tfrac{1739}{232243200}\,b^2+\tfrac{7639}{51030000}\,b^4+\tfrac{409}{58320000}\,b^6)\epsilon^7\\
&+(\tfrac{11}{5733089280}-\tfrac{67}{470292480}\,b^2-\tfrac{19979}{261273600}\,b^4-\tfrac{864931}{48988800000}\,b^6\\
&-\tfrac{60703}{489888000000}\,b^8)\epsilon^8+O(\epsilon^9),
\end{aligned}\tag{2.21}$$

$$\begin{aligned}
\lambda_3' \;=\;& 9+(\tfrac{9}{64}+\tfrac{9}{70}b^2)\epsilon^2-\tfrac{3}{512}\epsilon^3+(\tfrac{9}{65536}+\tfrac{9}{4480}\,b^2+\tfrac{279}{1372000}\,b^4)\epsilon^4\\
&+(\tfrac{15}{524288}-\tfrac{1311}{1254400}\,b^2-\tfrac{3}{12800}\,b^4)\epsilon^5\\
&+(-\tfrac{141}{33554432}+\tfrac{3207}{50462720}\,b^2+\tfrac{17789}{351232000}\,b^4+\tfrac{5953}{10084200000}\,b^6)\epsilon^6\\
&+(-\tfrac{21}{536870912}+\tfrac{19287}{1284505600}\,b^2-\tfrac{20945241}{786759680000}\,b^4-\tfrac{93}{31360000}\,b^6)\epsilon^7\\
&+(\tfrac{4101}{68719476736}-\tfrac{569953}{180858388480}\,b^2+\tfrac{6165641}{1186883174400}\,b^4+\tfrac{25654589}{28397107200000}\,b^6\\
&+\tfrac{171697}{316240512000000}\,b^8)\epsilon^8+O(\epsilon^9),
\end{aligned}\tag{2.22}$$

$$\begin{aligned}
\lambda_4' \;=\;& 9+(\tfrac{9}{64}+\tfrac{9}{70}b^2)\epsilon^2+\tfrac{3}{512}\epsilon^3+(\tfrac{9}{65536}+\tfrac{9}{4480}\,b^2+\tfrac{279}{1372000}\,b^4)\epsilon^4\\
&-(\tfrac{15}{524288}-\tfrac{1311}{1254400}\,b^2-\tfrac{3}{12800}\,b^4)\epsilon^5\\
&+(-\tfrac{141}{33554432}+\tfrac{3207}{50462720}\,b^2+\tfrac{17789}{351232000}\,b^4+\tfrac{5953}{10084200000}\,b^6)\epsilon^6\\
&-(-\tfrac{21}{536870912}+\tfrac{19287}{1284505600}\,b^2-\tfrac{20945241}{786759680000}\,b^4-\tfrac{93}{31360000}\,b^6)\epsilon^7\\
&+(\tfrac{4101}{68719476736}-\tfrac{569953}{180858388480}\,b^2+\tfrac{6165641}{1186883174400}\,b^4+\tfrac{25654589}{28397107200000}\,b^6\\
&+\tfrac{171697}{316240512000000}\,b^8)\epsilon^8+O(\epsilon^9),
\end{aligned}\tag{2.23}$$

$$\begin{aligned}
\lambda_3 \;=\;& 16+(\tfrac{2}{15}+\tfrac{8}{63}b^2)\epsilon^2+(\tfrac{11}{108000}+\tfrac{1}{945}\,b^2+\tfrac{59}{500094}\,b^4)\epsilon^4\\
&-\tfrac{25}{127008}b^2\epsilon^5+(\tfrac{1033}{1360800000}+\tfrac{58031}{5837832000}\,b^2+\tfrac{19363}{1584297792}\,b^4+\tfrac{19561}{218336039460}\,b^6)\epsilon^6\\
&-(\tfrac{1}{529200}\,b^2+\tfrac{61069}{6301184400}\,b^4+\tfrac{1}{1411200}\,b^6)\epsilon^7\\
&+(-\tfrac{60703}{31352832000000}+\tfrac{10021589}{73556683200000}\,b^2+\tfrac{2034457}{41191742592000}\,b^4+\tfrac{7397773}{74313648339840}\,b^6\\
&+\tfrac{41146789}{110921694798942720}\,b^8)\epsilon^8+O(\epsilon^9),
\end{aligned}\tag{2.24}$$

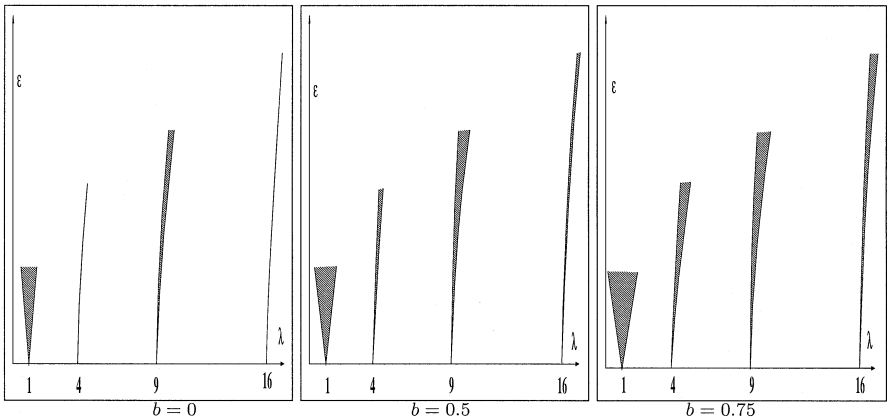

Figure 2. Stability diagram of Equation (2.17) for various value of b. The shaded regions are areas of instability. When $b = 0$ the instability areas have disappeared for $\lambda = 4n^2$.

$$\begin{aligned}\lambda_4 \;=\; & 16 + (\tfrac{2}{15} + \tfrac{8}{63}b^2)\epsilon^2 + (\tfrac{11}{108000} + \tfrac{1}{945}\,b^2 + \tfrac{59}{500094}\,b^4)\epsilon^4 \\ & + \tfrac{25}{127008}b^2\epsilon^5 + (\tfrac{1033}{1360800000} + \tfrac{58031}{5837832000}\,b^2 + \tfrac{19363}{1584297792}\,b^4 + \tfrac{19561}{218336039460}\,b^6)\epsilon^6 \\ & + (\tfrac{1}{529200}\,b^2 + \tfrac{61069}{6301184400}\,b^4 + \tfrac{1}{1411200}\,b^6)\epsilon^7 \\ & + (-\tfrac{60703}{31352832000000} + \tfrac{10021589}{73556683200000}\,b^2 + \tfrac{2034457}{41191742592000}\,b^4 + \tfrac{7397773}{74313648339840}\,b^6 \\ & + \tfrac{41146789}{110921694798942720}\,b^8)\epsilon^8 + O(\epsilon^9).\end{aligned} \tag{2.25}$$

One can easily check that for $b \to 0$ (2.18)–(2.25) reduce to (2.11)–(2.16). It can be shown that for $b \neq 0$ the stability diagram of Equation (2.17) has a similar geometry for ϵ small as the stability diagram of the Mathieu Equation (see Figure 1). The areas of instability depend on the parameter b in the coefficient of the damping term. As depicted in Figure 2, one may observe that, when b goes to zero, the areas of instability become narrower and finally when b equals zero the areas of instability vanish, especially for $\lambda = 4n^2$, $n = 1, 2, 3, \cdots$. This phenomenon has been described in [7, 8, 9] for an equation that differs from the one presented here.

3. An application in the theory of rain-wind-induced vibrations

In this section an application is given of the results obtained above. The application is concerned with the rain-wind-induced vibrations of a simple one-degree-of-freedom system related to the dynamics of cable-stayed bridges. Firstly it will be shown how to model this problem in order to obtain a model equation of the form (1.1). Cable-stayed bridges are characterized by inclined stay cables connecting the bridge deck with one or more pylons. Usually the stay cables have a smooth polyurethane mantle and a cross section which is nearly circular. Under normal circumstances for such type of cables one would not expect galloping vibrations due to wind forces. There are, however, exceptions: in the winter season ice accretion on the cable may induce aerodynamic instability resulting in vibrations with

relatively large amplitudes. The instability mechanism for this type of vibrations is known and can be understood on the basis of quasi-steady modeling and analysis. In this analysis the so-called Den Hartog criterion, expressing a condition for an unstable equilibrium state, plays an important part. The other exception concerns vibrations excited by a wind field containing raindrops. This phenomenon was probably detected for the first time by Japanese researchers, as can be derived from the papers by Matsumoto a.o. [10, 11]. As has been observed on scale models in wind tunnels, the raindrops that hit the inclined stay cable generate one or more rivulets on the surface of the cable. The presence of flowing water on the cable changes the cross-section of the cable as experienced by the wind field. Accordingly, the pressure distribution on the cable, with respect to the direction of the (uniform) wind flow, may become asymmetric, resulting in a lift force perpendicular to direction of the wind velocity.

It is of interest to remark that there is an important difference between the presence of ice accretion and rivulets as far as the dynamical behaviour is concerned. The ice accretion results in an ice coating fixed to the surface of the cable, whereas the rivulet leads a flow of water on the surface of the cable where the position of the rivulet depends on the resulting wind velocity, the surface tension of the water and the adhesion between the water and polyurethane mantle of the cable.

For the interesting cases the thickness of the ice accretion is not uniform: the evolution process of ice accretion usually results in an ice coating involving a ridge of ice. The case with water rivulets can also be characterized by the presence of the ridge of water, be it with the difference that this water ridge is not fixed to the surface of the cable. As long as the water ridge is present, it may be blown off if the wind speed exceeds a critical value, one may assume that the position of the ridge varies in time. This is a conclusion given in the paper by Ruscheweyh [12], where it is remarked that the rhythmic movement of the water rivulets, cable and aerodynamic force seem to be the key point for understanding the phenomenon. One may assume that this time-dependence has a character similar to the motion of the cable, *i.e.*, if the cable oscillates harmonically, then one may expect that the water ridge moves accordingly. The observation of this complicated system of an inclined cable, connecting a bridge deck and a pylon with a moving rivulet, leads to the following conclusion.

The inclination of the cable is relevant for having a rivulet. The rivulet, however, can be viewed as a moving ridge that may be modeled by a solid state. According to this way of modeling, the inclination of the cable is no longer relevant. Hence we consider as a prototype of an oscillator a one-degree-of-freedom system consisting of a horizontal rigid cable supported by springs with a solid-state ridge moving with small-amplitude oscillations. From the point of view of the type of equation of motion, we arrive at a second-order differential equation with external forcing. A more detailed description of the modeling is presented in the following section.

3.1. The model equation for rain-wind-induced vibrations of a prototype oscillator

The modeling principles we use are closely related to the quasi-steady approach as given in [13]. We consider a rigid cylinder with uniform cross-section supported by springs in a uniform rain-wind flow directed perpendicularly to the axis of the cylinder. The oscillator is constructed in such a way that only vertical (one degree of freedom) oscillations are possible. The basic cross-section of the cylinder is circular; however, on the surface of the cylinder there is a ridge that can carry out small-amplitude oscillations. To model the rain-wind forces on the

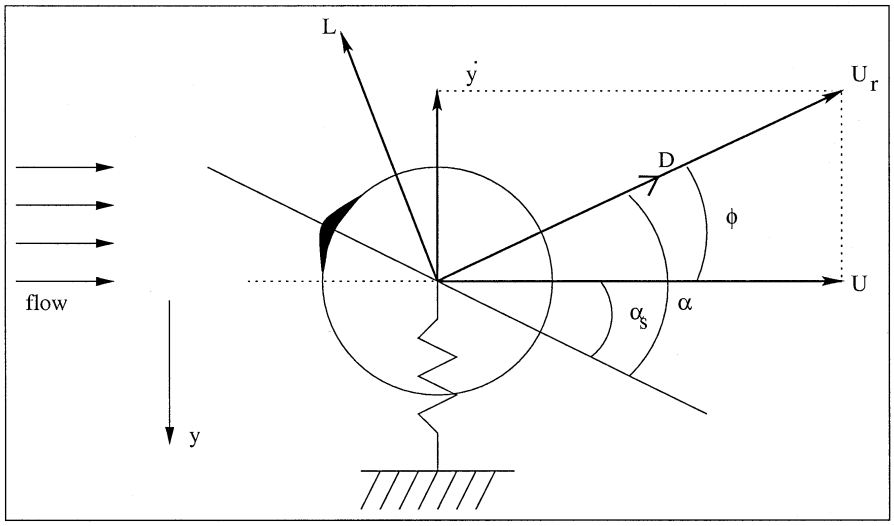

Figure 3. Cross-section of the cylinder-spring system, fluid flow with respect to the cylinder and wind forces on the cylinder.

cylinder, a quasi-steady approach is used; the type of oscillations that can be studied subject to the respective assumptions are known as galloping. A more detailed description of the quasi-steady approach can be found in [14, 15]. The basic assumption of the quasi-steady approach is that, at each moment in the dynamic situation, the rain-wind force can be taken equal to the steady force exerted on the cylinder in static state. In the dynamic situation one should take into account that the flow-induced forces are based on the instantaneous flow velocity which is equal to the vector sum of flow velocity and the time varying vertical flow velocity induced by the (vertical) motion of the cylinder.

The steady rain-wind forces can be measured in a wind tunnel and are expressed in the form of non-dimensional aerodynamic coefficients depending on the angle of attack α. This angle, which is an essential variable for the description of the dynamics of the oscillator, is defined as the angle between the resultant flow velocity and a reference axis fixed to the cylinder and measured positive in a clockwise direction. The system we will study in more detail is sketched in Figure 3. The horizontal wind velocity is U and, as the cylinder is assumed to move in the positive y-direction, there is a virtual vertical wind velocity $-\dot{y}$. The drag force D is indicated in the direction of the resultant wind velocity U_r, whereas the lift force L is perpendicular to D in an anti-clockwise direction. The shaded ridge on the cylinder is indicated in Figure 3 and is able to carry out small-amplitude oscillations. The vertical aerodynamic force F_y can easily be derived from Figure 3:

$$F_y = -D \sin\phi - L \cos\phi, \tag{3.1}$$

where ϕ is the angle between U_r and U, positive in clockwise direction, with $|\phi| \leq \pi/2$. The drag and lift force are given by the empirical relations:

$$D = \frac{1}{2}\rho\, d\, l\, U_r^2\, C_D(\alpha), \qquad L = \frac{1}{2}\rho\, d\, l\, U_r^2\, C_L(\alpha), \tag{3.2}$$

where ρ is the density of air, d the diameter of the cylinder, l the length of the cylinder, $C_D(\alpha)$ and $C_L(\alpha)$ are the drag and lift coefficient curves respectively, determined by measurements in a wind-tunnel.

From Figure 3 it follows that:

$$\sin\phi = \dot{y}/U_r, \qquad \cos\phi = U/U_r, \qquad \alpha = \alpha_s + \arctan(\dot{y}/U). \tag{3.3}$$

The equation of motion of the oscillator readily becomes :

$$m\ddot{y} + c_y\dot{y} + k_y y = F_y, \tag{3.4}$$

where m is the mass of the cylinder, $c_y > 0$ the structural-damping coefficient of the oscillator, $k_y > 0$ the spring constant.

By using (3.2) and (3.3) we obtain for F_y:

$$F_y = -\frac{1}{2}\rho\, d\, l\sqrt{U^2 + \dot{y}^2}\,(C_D(\alpha)\dot{y} + C_L(\alpha)U). \tag{3.5}$$

By setting $\omega_y^2 = k_y/m$, $\tau = \omega_y t$ and $z = \omega_y y/U$ Equation (3.4) becomes:

$$\ddot{z} + 2\beta\dot{z} + z = -K\sqrt{1+\dot{z}^2}\,(C_D(\alpha)\dot{z} + C_L(\alpha)), \qquad \alpha = \alpha_s + \arctan(\dot{z}), \tag{3.6}$$

where $2\beta = c_y/m\omega_y$ and $K = \rho\, d\, lU/2m\omega_y$ are non-dimensional parameters, and $\dot{z}$ now stands for differentiation with respect to τ.

We study the case where the drag- and lift-coefficient curve can be approximated by a constant and a cubic polynomial respectively:

$$C_D(\alpha) = C_{D_o}, \qquad C_L(\alpha) = C_{L_1}(\alpha - \alpha_o) + C_{L_3}(\alpha - \alpha_o)^3, \tag{3.7}$$

where $C_{D_o} > 0$ and for the interesting cases $C_{L_1} < 0$ and $C_{L_3} > 0$. By using $\alpha = \alpha_s + \arctan\dot{z}$, we obtain for $C_L(\alpha)$:

$$C_L(\alpha) = C_{L_1}(\alpha_s - \alpha_o + \arctan\dot{z}) + C_{L_3}(\alpha_s - \alpha_o + \arctan\dot{z})^3. \tag{3.8}$$

The cases $\alpha_s = \alpha_o$ and $\alpha_s \neq \alpha_o$, where α_s and α_o are (time independent) parameters, have been studied in [13]. Here we study the case that the position of the (water) ridge varies with time:

$$\alpha_s - \alpha_o = f(t) = f(\tau/\omega_y). \tag{3.9}$$

Substitution of (3.8) and (3.9) in (3.6) and expanding the right hand side with respect to $\dot{z}$ in the neighbourhood of $\dot{z} = 0$ yields:

$$\begin{aligned}\ddot{z} + z \;=\; & -K[C_{L_1}f(t) + C_{L_3}f^3(t) + (C_{D_o} + C_{L_1} + 2\beta/K + 3C_{L_3}f^2(t))\,\dot{z} + \\ & (\frac{1}{2}C_{L_1}f(t) + \frac{1}{2}C_{L_3}f^3(t) + 3C_{L_3}f(t))\,\dot{z}^2 + \\ & (\frac{1}{6}C_{L_1} + C_{L_3} + \frac{1}{2}C_{D_o} + \frac{1}{2}C_{L_3}f^2(t))\,\dot{z}^3] + 0(\dot{z}^4).\end{aligned} \tag{3.10}$$

Inspection of this equation shows that for $f(t) \equiv 0$ one obtains:

$$\ddot{z} + z = K[-(C_{D_o} + C_{L_1} + 2\beta/K)\,\dot{z} - (\frac{1}{6}C_{L_1} + C_{L_3} + \frac{1}{2}C_{D_o})\,\dot{z}^3]. \tag{3.11}$$

When the following conditions hold :

$$C_{D_o} + C_{L_1} + 2\beta/K < 0 \text{ (Den Hartog's Criterion)}, \quad \frac{1}{6}C_{L_1} + C_{L_3} + \frac{1}{2}C_{D_o} > 0, \tag{3.12}$$

the equation can be reduced to the Rayleigh equation, which has, as is well-known, a unique periodic solution (limit-cycle). The linearized version of Equation (3.11) has, apart from $z \equiv 0$, only unbounded solutions if Den Hartog's criterion applies. Linearization of Equation (3.10), however, leads to an equation that may have periodic solutions and is hence of interest to study in more detail.

The linearized version of (3.10) can be written as :

$$\ddot{z} + K(C_{D_o} + C_{L_1} + 2\beta/K + 3C_{L_3} f^2(t))\,\dot{z} + z + K(C_{L_1} f(t) + C_{L_3} f^3(t)) = 0. \quad (3.13)$$

We consider the case that $f(t) = A\cos\omega t = A\cos(\frac{\omega}{\omega_y}\tau) = A\cos\Omega\tau$ where $\Omega = \frac{\omega}{\omega_y}$ with

$$f^2(t) = \frac{1}{2}A^2(1 + \cos 2\Omega\tau) \qquad \text{and} \qquad f^3(t) = \frac{3}{4}A^3(\cos\Omega\tau + \frac{1}{3}\cos 3\Omega\tau).$$

Equation (3.13) becomes:

$$\ddot{z} + (KA_o + KA_1\cos 2\Omega\tau)\,\dot{z} + z + KA_2\cos\Omega\tau + KA_3\cos 3\Omega\tau = 0, \quad (3.14)$$

where

$$A_o = C_{D_o} + C_{L_1} + 2\beta/K + \frac{3}{2}C_{L_3}A^2, \qquad A_1 = \frac{3}{2}C_{L_3}A^2,$$
$$A_2 = C_{L_1}A + \frac{3}{4}C_{L_3}A^3, \qquad A_3 = \frac{1}{4}C_{L_3}A^3.$$

For the oscillator we study the interesting case $\Omega = 1 + \epsilon\eta$ where $|\epsilon| \ll 1$. If we set $(1 + \epsilon\eta)\tau = \theta$, (3.14) becomes:

$$(1+\epsilon\eta)^2\,\ddot{z} + (1+\epsilon\eta)(KA_o + KA_1\cos 2\theta)\,\dot{z} + z + KA_2\cos\theta + KA_3\cos 3\theta = 0, \quad (3.15)$$

where a dot now stands for differentiation with respect to θ.

Let the coefficients KA_i $i = 0, 1, 2, 3$ be of $O(\epsilon)$. Then (3.15) can be written as:

$$\ddot{z} + (KA_o + KA_1\cos 2\theta)\,\dot{z} + (1 - 2\epsilon\eta)z + KA_2\cos\theta + KA_3\cos 3\theta + O(\epsilon^2) = 0. \quad (3.16)$$

If one neglects the $O(\epsilon^2)$ term then the only difference between Equation (3.16) and Equation (1.1) (for $m = 1$) is the term $KA_3\cos 3\theta$. This term can be regarded as a forcing term, but as the frequency is three times greater than the natural frequency, it is not relevant for the $O(\epsilon)$ approximation. Putting $KA_o = a_o\epsilon$, $KA_1 = a_1\epsilon$, $KA_2 = a_2\epsilon$, and $KA_3 = a_3\epsilon$ and neglecting $O(\epsilon^2)$ of (3.16) one obtains:

$$\ddot{z} + \epsilon(a_o + a_1\cos 2\theta)\,\dot{z} + (1 - 2\epsilon\eta)z + a_2\cos\theta + a_3\cos 3\theta = 0. \quad (3.17)$$

Transforming (3.17) by new variables y_1 and y_2, *i.e.*,

$$z = y_1\cos\theta + y_2\sin\theta, \qquad \dot{z} = -y_1\sin\theta + y_2\cos\theta, \quad (3.18)$$

one obtains by averaging:

$$\begin{pmatrix} \dot{\bar{y}}_1 \\ \dot{\bar{y}}_2 \end{pmatrix} = \epsilon \begin{pmatrix} -\frac{1}{2}a_o + \frac{1}{4}a_1 & -\eta \\ \eta & -\frac{1}{2}a_o - \frac{1}{4}a_1 \end{pmatrix} \begin{pmatrix} \bar{y}_1 \\ \bar{y}_2 \end{pmatrix} + \epsilon \begin{pmatrix} 0 \\ -\frac{1}{2}a_1 \end{pmatrix}. \quad (3.19)$$

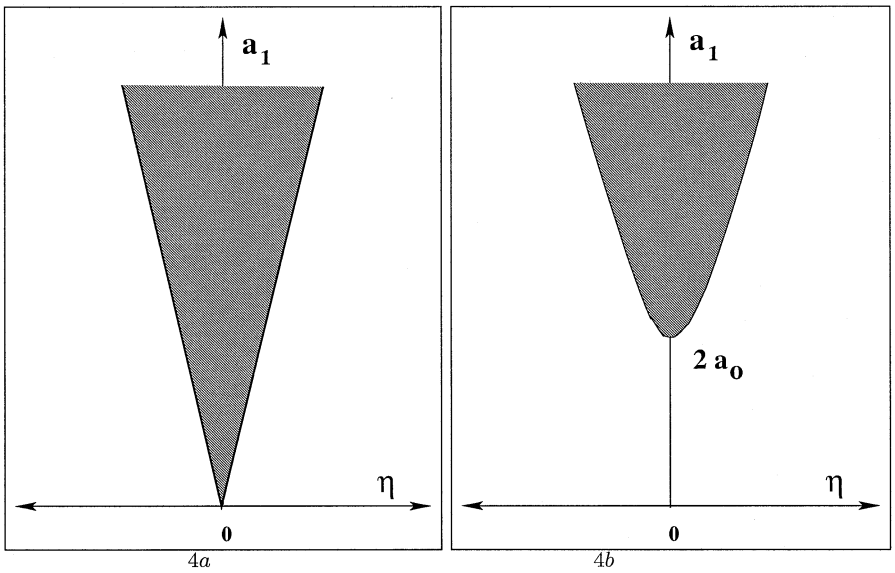

Figure 4. Separation of the instability tongue: Figure 4a: $a_o = 0$; Figure 4b: $a_o > 0$.

The critical point of (3.19) is

$$\left(\frac{\frac{1}{2}\eta a_2}{\frac{1}{4}a_o^2 - \frac{1}{16}a_1^2 + \eta^2}, \quad \frac{\frac{1}{2}a_2(-\frac{1}{2}a_o + \frac{1}{4}a_1)}{\frac{1}{4}a_o^2 - \frac{1}{16}a_1^2 + \eta^2} \right).$$

If the determinant of the coefficient matrix of (3.19) is not equal to zero, then (3.17) has a periodic solution and its stability depends on the eigenvalues of the coefficient matrix . The eigenvalues of the coefficient matrix are

$$\frac{1}{2}\epsilon \left(-a_o \pm \sqrt{\frac{1}{4}a_1^2 - 4\eta^2} \quad \right).$$

By equating these eigenvalues to zero one obtains the transition curves between the stable and unstable regions $a_o = \sqrt{\frac{1}{4}a_1^2 - 4\eta^2}$ in the (a_1, η) plane. For $a_o = 0$ the stability diagram is depicted in Figure 4a and if $a_o > 0$ the instability area is separated from the η-axis by a distance $2a_o$ as shown in Figure 4b. In a similar way the instability tongues are separated from the η-axis for $\lambda = (2n + 1)^2$ $n = 0, 1, 2, \cdots$. Additionally, it can be shown that for $\lambda = 4n^2$ the curves of coexistence of periodic solutions disappear for $a_o > 0$.

4. Conclusions

In this paper a linear second-order equation with time-periodic damping coefficient has been investigated. It has been shown that the equation can be used as a model for studying rain-wind-induced vibrations of a simple oscillator. The equation is a special case of Ince's equation. It has been known that this equation displays coexistence, corresponding with curves in the stability diagram on which two linearly independent periodic solutions exist. These curves can be considered as a limiting case of the closure of instability gaps. Although this phenomenon has been described in [3] in qualitative sense, little quantitative results such as

stability diagrams have been obtained. A new remarkable stability diagram is presented in Figure 1b; for small values of ϵ the (transition) curves are additionally given by (truncated) power series in ϵ. As far as the application is concerned, it seems that only one application has been published yet so far [8]. The application presented here seems to be new and is of practical relevance. Problems with a time-varying damping coefficient play a role in the dynamics of rain-wind-induced vibrations of elastic structures and are hence of considerable interest. To evaluate the model equation, laboratory experiments could be set up with a time-varying electromagnetic damping device. Finally, one may conclude that now the way looks open to investigate more-complicated oscillators, including ones with two or more degrees of freedom.

References

1. D.B. Batchelor, Parametric resonance of systems with time-varying dissipation. *Appl. Phys. Lett.* 29 (1976) 280–281.
2. Hartono and A.H.P. van der Burgh, Periodic solutions of an inhomogeneous second order equation with time-dependent damping coefficient, In: Sinha *et al.* (eds.), *Proceeding the 18th Biennial ASME Conference, September 9-12, 2001 Pittsburgh USA, Symposium on Dynamics and Control of Time-Varying Systems and Structures.* New York: ASME (2001) Vol. DETC2001/VIB-21415 pp. 1–8.
3. W. Magnus and S. Winkler, *Hill's Equation.* New York: John Wiley & Sons (1966) 127 pp.
4. H. Hochstadt, A direct and inverse problem for a Hill's equation with double Eigenvalues. *J. Math. Anal. Appl.* 66 (1978) 507–513.
5. R. Grimshaw, *Nonlinear Ordinary Differential Equations.* Boca Raton: CRC Press (1993) 328 pp.
6. A.H. Nayfeh and D.T. Mook, *Nonlinear Oscillations.* New York: John Wiley & Sons (1995) 704 pp.
7. R.H. Rand and S.F. Tseng, On the stability of a differential equation with application to the vibrations of a particle in the plane. *J. Appl. Mech.* June (1969) 311–313.
8. R.H. Rand and S.F. Tseng, On the Stability of the vibrations of a particle in the plane restrained by two non-identical springs. *Int. J. Non-Lin. Mech.* 5 (1970) 1–9.
9. N.G. Leslie and R.H. Rand, Nonlinear effects on coexistence phenomenon in parametric excitation. *Nonlin. Dyn.* 31 (2003) 73–89.
10. M. Matsumoto, N. Shiraishi, M. Kitazawa, C. Knisely, H. Shirato, Y. Kim and M. Tsujii, Aerodynamic behavior of inclined circular cylinders-cable aerodynamics. *J. Wind Engng. Industr. Aerodyn.* 33 (1990) 63–72.
11. M. Matsumoto, M. Yamagishi, J. Aoki and N. Shiraishi, Various mechanism of inclined cable aerodynamics. In: *International Association for Wind Engineering Ninth International Conference on Wind Engineering.* New Dehli: New Age International Publishers Limited Wiley Eastern Limited (1995) Vol. 2 pp. 759–770.
12. C. Verwiebe and H. Ruscheweyh, Recent research results concerning the exciting mechanism of rain-wind induced vibrations. In: G. Solari (ed.), *Proceeding 2nd European and African Conference on Wind Engineering.* Padova: SGE (1997) pp. 1783-1790.
13. T.I. Haaker and A.H.P. van der Burgh, On the dynamics of aeroelastic oscillators with one degree of freedom. *SIAM J. Appl. Math.* 54 (1994) 1033–1047.
14. A.H.P. van der Burgh, Nonlinear dynamics of structures excited by flows: quasi-steady modeling and asymptotic analysis. In: H. Dominique (ed.), *Fluid-Structure Interactions in Acoustics.* New York: Springer Wien (1999) pp. 221–259.
15. A.H.P. van der Burgh, Rain-wind induced vibrations of a simple oscillator. In: Sinha *et al.* (eds.), *Proceeding for the 18th Biennial ASME Conference, Symposium on Dynamics and Control of Time-Varying Systems and Structures.* New York: ASME (2001) Vol. DETC2001/VIB-21429 pp. 1–6.
16. J.A. Sanders and F. Verhulst, *Averaging Methods in Nonlinear Dynamical Systems.* New York: Springer-Verlag (1985) 247 pp.